The Third Parameter in Reactive Barrier Films

Eric E. Nuxoll and E. L. Cussler
Dept. of Chemical Engineering & Materials Science, University of Minnesota, Minneapolis, MN 55455

DOI 10.1002/aic.10316
Published online in Wiley InterScience (www.interscience.wiley.com).

The lag time of a barrier film can be dramatically increased by the addition of sacrificial scavengers that consume solute before crossing the barrier. This increase in lag time is independent of the scavengers' reaction rate. This reaction rate does affect the amount of solute that crosses the membrane before steady state, a premature leakage that may render the barrier unsuitable regardless of its putative lag time and permeability. A third parameter is needed to characterize the barrier's transient behavior. Guided by experiments, we offer two candidate parameters for quantifying these changes. Correlations of these parameters are determined numerically and compared with experimental results. © 2005 American Institute of Chemical Engineers *AIChE J,* 51: 456–463, 2005
Keywords: barrier membranes, reactive membranes, lag time, leakage, kill time

Introduction

Barrier membranes are films that block a target solute from crossing them. Such barriers can keep oxygen out of food, chlorinated solvents out of aquifers, and corrosives away from cars. This imperviousness to the target solute is often balanced against other properties, such as cost, ductility, environmental impact, and desirable permeability to other solutes. Improving the barrier quality of materials with other attractive properties is an ongoing effort, and this paper explores the details of one such effort: adding reactive scavenging groups to the material.

Commonly, the quality of a barrier is characterized by two parameters, the permeability and the lag time. The physical meaning of these two parameters can be understood from the following experiment. Imagine that the membrane, with thickness ℓ and area A, protects a substrate from target solute X, present on the other side of the membrane at a constant concentration C_{X0}. The membrane is initially devoid of solute and the substrate acts as a perfect sink. If the mass-transfer resistance at the interfaces is negligible, the total amount of solute reaching the substrate Q will vary with time t as follows[1]:

$$Q = \frac{ADHC_{X0}}{\ell}\left[t - \frac{\ell^2}{6D} - \frac{2\ell^2}{\pi^2 D}\sum_{n=1}^{\infty}\frac{(-1)^2}{n^2}\exp\left(\frac{-Dn^2\pi^2 t}{\ell^2}\right)\right] \tag{1}$$

where D is the diffusion coefficient of solute in the membrane, and H is its partition coefficient; both are assumed to be constant. Except at the smallest times, the summation in Eq. 1 approaches zero, and the equation reduces to[2]

$$Q = \frac{ADHC_{X0}}{\ell}\left(t - \frac{\ell^2}{6D}\right) \tag{2}$$

This asymptote mathematically defines the first two parameters of barrier quality: the permeability and the lag time. After factoring out the geometry (A/ℓ) and the driving force (C_{X0}), the slope gives the permeability, DH. The intercept on the time axis is the mathematical definition of the membrane's lag time, t_L. For barrier membranes, we want the permeability to be as small as possible and the lag time to be as large as possible.

For nonreactive films, the lag time is often so short it is ignored. However, the lag time can be increased by orders of magnitude by adding a sacrificial scavenger to the membrane. By "sacrificial scavenger," we mean a reagent that is consumed, rather than a catalyst that simply alters the reaction rate. At the same time, the scavenger consumes the solute as the solute diffuses through the membrane, destroying it before it can reach the substrate. After the scavenger is depleted, the solute will diffuse through the membrane just as it would had the scavenger never been present. The permeability of the membrane is unchanged, whereas the lag time increases dramatically because large amounts of solute must diffuse into the film before the scavenger is depleted and steady-state flux can begin.

Correspondence concerning this article should be addressed to E. L. Cussler at cussler@cems.umn.edu

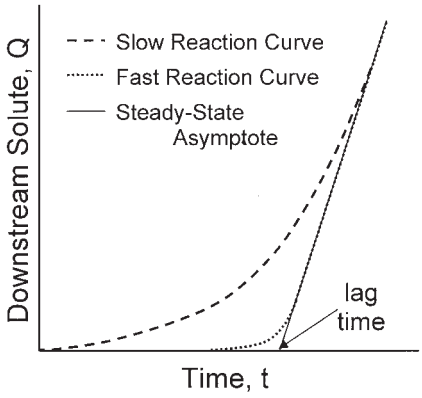

Figure 1. Breakthrough curves for reactive membranes that differ only in their reaction rate (the leakage changes whereas the lag time does not).

The increased lag time, which has frequently been estimated[3-10] for irreversible reactions, is equal to

$$t_L = \frac{\ell^2}{6D}\left(1 + \frac{3C_{Y0}}{\nu H C_{X0}}\right) \tag{3}$$

where C_{Y0} is the initial concentration of scavenger in the membrane and ν is a stoichiometric constant (that is, $X + \nu Y \rightarrow$ Product). Because the term in parentheses in Eq. 3 can be of order 1000, a film that previously had a lag time of 1 week can be given a lag time of decades. Thus for reactive barrier membranes, the lag time is often more important than the permeability.

For the sacrificial scavengers addressed in this article, the observed permeability is independent of the reaction rate. This independence, demonstrated numerically[10] and analytically,[3] underscores the fact that both the lag time and the permeability are steady-state parameters, determined by a steady-state breakthrough asymptote. Because the asymptote does not occur until after reaction has ceased, we should not expect the asymptote to reflect its rate.

What effect does the reaction rate have in these systems? The answer appears in the transient portion of the barrier's breakthrough curve. Although barriers of different reaction rates may approach the same asymptote, they will approach it by different paths. If the reaction is instantaneous, then the moment a solute molecule reaches the scavenger-rich region of the membrane, the solute and scavenger annihilate each other. In this scenario, the solute slowly eats its way across the film, developing a concentration profile along the way. When the solute reaches the downstream interface, all of the scavenger has been consumed and the linear, steady-state concentration profile is in place. Steady-state solute flux into the package then begins immediately, as shown in the dotted line in Figure 1. This is the scenario we described above.

However, we are also interested in cases where the reaction is slower. In many applications there are substantial penalties for accelerating the reaction rate of the scavenger. Any catalyst needed may be expensive and environmentally regulated. Aggressive scavengers may also degrade the barrier matrix and increase the permeability. In these cases, we may question whether the accelerated rate is worth the cost. If the reaction rate is slow, some solute may diffuse past the scavenger and into the package before it is consumed. The amount of solute Q begins to increase almost immediately and only slowly approaches the steady-state asymptote as the scavenger is depleted. This is shown by the dashed line in Figure 1.

If enough solute leaks through, the effectiveness of the barrier may be compromised long before the lag time is reached. Neither the permeability nor the lag time, both steady-state parameters, offer any suggestion of this premature demise. To evaluate the consequences of a slower reaction rate, a third parameter is needed to quantify this transient solute flux. This paper seeks this third parameter.

We study the effect of slow reaction both by experiment and by theory. The experiments use the same acid/base reaction as previous studies,[10,11] where immobilized ZnO consumes HCl as it diffuses across a polyvinyl alcohol (PVA) membrane. Of course, if the ZnO and HCl could be well mixed, their reaction would be instantaneous. Because ZnO is solid, the effective reaction rate is limited by diffusion of HCl from the bulk polymer to the surface of the zinc oxide particles.

We use this reaction heterogeneity to adjust the apparent reaction rate. In particular, we take advantage of the fact that the apparent reaction rate for this system is[12]

$$\left[\frac{\text{reaction}}{\text{volume}}\right] = \left\{\frac{3\phi D}{R^2}\right\} C_X \tag{4}$$

where ϕ is the initial volume fraction of ZnO, D is the diffusion coefficient of the HCl, R is the ZnO particle radius, and C_X is the HCl concentration in the bulk polymer. Note that this implies that we can change the apparent first-order reaction rate (in braces in Eq. 4) simply by changing the particle size. Larger particles at a constant volume fraction ϕ means fewer particles, with less overall surface area and longer diffusion paths to this area. Diffusion from the bulk polymer, where the HCl concentration is C_X, to the particle surface, where the HCl concentration is zero, takes longer. Thus the apparent reaction is slower.

Experimental

To explore the effects of reaction rate experimentally, we adapted the system that Yang et al.[10] used for the experimental confirmation of the instantaneous reaction limit summarized by Eq. 3. Zinc oxide immobilized in PVA forms an effective barrier to acids, as the ZnO consumes acid permeating the film in accordance with the following equation

$$\mathrm{HCl} + \tfrac{1}{2}\mathrm{ZnO} \rightarrow \tfrac{1}{2}\mathrm{H_2O} + \tfrac{1}{2}\mathrm{ZnCl_2} \tag{5}$$

ZnO particles of different sizes were used to change the effective reaction rate of the system.

To obtain different particle sizes, a 13% (w/w) slurry of ZnO (Zinox 350, American Chemet) in water was sent through a 1-in. hydrocyclone (Richard Mozley, Ltd.) with a 7.0-mm vortex finder and 2.2-mm spigot at 350-kPa gauge pressure to fractionate ZnO particles according to size. The tops (predominantly smaller particles) and bottoms (predominantly larger particles) were rerun under the same conditions. The second

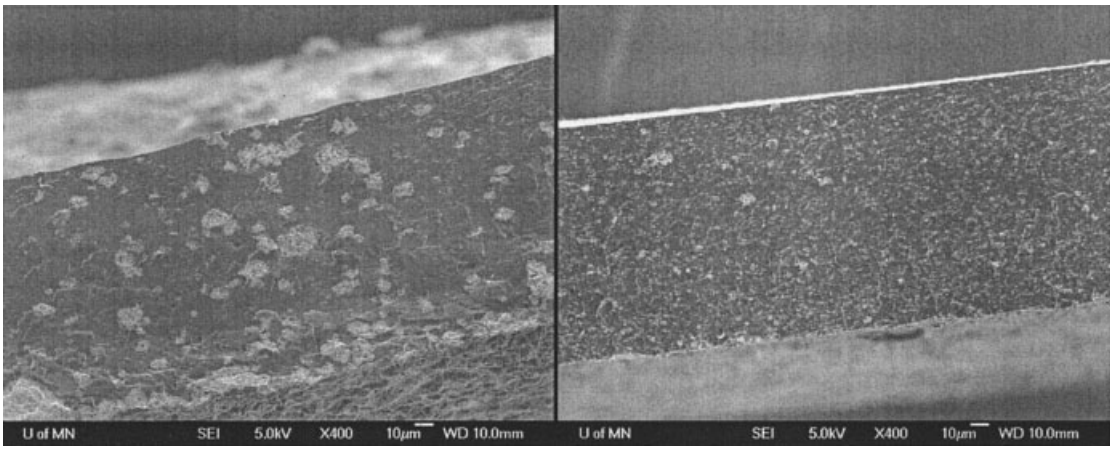

Figure 2. SEM images of cross sections of PVA membranes with large (left image) and small (right image) ZnO particles (ZnO particles appear white against dark PVA matrices).

generation tops were left to agglomerate and settle overnight. Clear water was decanted from above the particles before storage. The second-generation bottoms were filtered into a cake and stored until use. ZnO was resuspended in water before use by stirring. Resuspension was performed by stirring overnight until the discovery that the stirring duration affected the resulting particle size, breaking apart the particles over time. Subsequent experiments showed that 30 min of stirring could resuspend particles with less breakup.

We report here on barrier membranes with four ZnO preparations: ZnO tops stirred overnight, ZnO bottoms stirred overnight, ZnO tops stirred 30 min, and ZnO bottoms stirred 30 min. The latter preparation was used in membranes with both typical (~3% v/v) and low (~1% v/v) ZnO content. Agglomeration made particle size analysis by light scattering qualitatively valuable at best; SEM images of the 30-min preparations within membranes are shown in Figure 2. Images of the overnight preparations are similar, but with smaller particles that differ less in size between tops and bottoms.

For each of the barrier membranes, 4.0 g PVA (Dupont Elvanol 71-30) was dissolved in 36 mL water by agitation and heating, and then degassed under vacuum. ZnO slurry was also degassed and added to the PVA solution. After stirring for 1 h, the mixture was poured onto a Teflon block and leveled to a uniform thickness of 1875 μm by a 10-cm doctor blade (Mitutoyo). Four milliliters of 0.0066 M $Na_2B_4O_7$ (Fisher) were stirred into the large particle solutions to increase their viscosity before pouring. These large-particle mixtures were also placed on a heating plate at 45°C to dry them before their particles could settle. The small-particle membranes were dried overnight at room temperature.

Once dried, each membrane was peeled from its Teflon block and heated to 150°C for 135 min for crosslinking.[13] Once cool, each membrane was placed in water overnight to hydrate, inspected for defects, and cut into circular samples 5 cm in diameter. Samples were tested in a diaphragm cell as described previously, generating breakthrough curves of downstream acid (HCl, Mallinckrodt) concentration vs. time.[10,11]

Although the ZnO content of each membrane could be precisely determined, it could not be as precisely controlled because differing amounts of ZnO slurry would stick to the stirring beaker. Similarly, the thickness from membrane to membrane varied (160–230 μm) as a result of changes in solids content and mixture viscosity. The thickness of samples within a given membrane was uniform [relative standard deviation (RSD) ~ 6%]. The permeability of the membranes is quite sensitive to the crosslinking step, with an RSD of 26%.

Experimental Results: Breakthrough Curves

Breakthrough curves for each preparation of membrane are given in Figures 3–5. Figure 3 compares membranes with ZnO stirred overnight, Figure 4 compares membranes with ZnO stirred 30 min, and Figure 5 compares membranes with different amounts of identical 30-min ZnO bottoms. Because slight differences in the steady-state asymptote of each breakthrough plot make direct comparisons of curvature difficult, the curves have been normalized to a common asymptote as follows. For each curve, Q is multiplied by the curve's asymptotic slope ($ADHC_{X0}/\ell$), according to Eq. 2, and the curve's lag time is subtracted from the time t. This

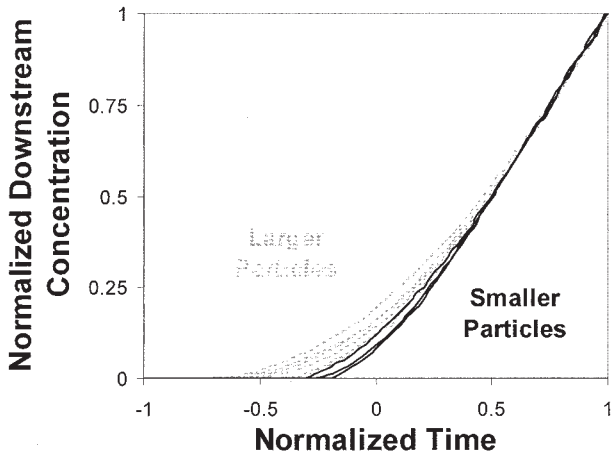

Figure 3. Normalized breakthrough curves for membranes with large (gray) and small (black) ZnO particles, each slurried overnight before incorporation in membrane.

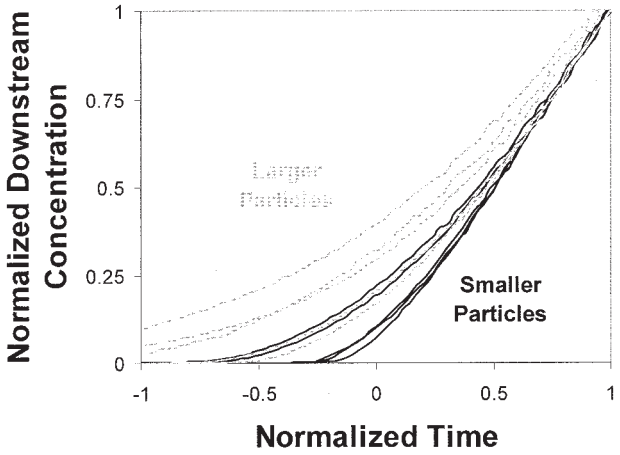

Figure 4. Normalized breakthrough curves for membranes with large (gray) and small (black) ZnO particles, each slurried for 30 min before incorporation in membrane.

Variation in particle size, and in resultant breakthrough curves, is more pronounced.

gives each normalized curve an asymptotic slope of one and an intercept of zero. Both axes were also multiplied by ℓ^2/D to make them dimensionless. Each set of curves represents samples cut from a single membrane, their variation in curvature indicative of the noise associated with second derivatives of experimental data.

Figures 3 and 4 show qualitatively that larger particles yield breakthrough curves with more curvature. Figure 5 shows that scavenger quantity also has a strong effect on the curvature, with more scavenger yielding more curvature. Thus the same membrane chemistry gives different curvature because of different effective reaction kinetics, as suggested by Figure 1. The barriers have different leaks and thus differ in their effectiveness; thus we cannot describe barrier effectiveness with only a permeability and lag time.

Analytical Results: Leakage and Kill Time

Up to now, we have spoken about the amount of curvature qualitatively because we have lacked the framework for evaluating it quantitatively. In other words, we do not know what third parameter to use beyond the permeability and the lag time. Now we offer two candidate parameters that are measures of a breakthrough curve's curvature: the leakage (L) and the kill time (t_K).

The leakage L is defined as the integral of Q over time for a given membrane minus the same integral for an ideal membrane with the breakthrough asymptote (that is, with zero curvature)

$$L = \int_0^\infty Q dt - \int_{t_L}^\infty \frac{ADHC_{X0}}{\ell}(t - t_L)dt \tag{6}$$

Referring back to Figure 1, we see that the leakage of the slow-reacting membrane is the area bounded by its dashed curve, the abscissa, and the steady-state asymptote. This area (and thus this leakage) is larger than that of the fast-reacting membrane whose dashed curve deviates much less from the asymptote.

This parameter is appropriate for products that degrade slowly over time. For instance, butter cookies do not instantly decompose in oxygen, but rather oxidize slowly. The rate at which they oxidize is a function of the amount of oxygen around them (that is, of Q). The amount of oxidation is the integral of this rate over time, so integrating Q over time would provide a measure of how much the butter cookies have oxidized. Because this integral will go to infinity as t goes to infinity, we subtract the integral of the "ideal" breakthrough curve, the steady-state asymptote that the real breakthrough curve will approach. This parameter would have to be considered in conjunction with the lag time and the permeability to determine a given membrane's suitability.

An alternative to the leakage is the kill time t_K, defined as the time required to reach a given critical value Q_{Max}. This parameter is a good choice to describe products that degrade quickly, such as the filament of an electric light bulb. As soon as enough oxygen has entered to package to erode the filament, the filament is dead. This parameter can be used alone to determine the suitability of a membrane, but depends on an additional arbitrary parameter Q_{Max}, and so is more complicated to model.

To predict the leakage and kill time, we start with mass balances where an immobile scavenger homogeneously dissolved into the membrane consumes solute in a second-order reaction with rate constant k

$$\frac{\partial C_X}{\partial t} = D\frac{\partial^2 C_X}{\partial z^2} - kC_XC_Y \tag{7}$$

$$\frac{\partial C_Y}{\partial t} = -\nu kC_XC_Y \tag{8}$$

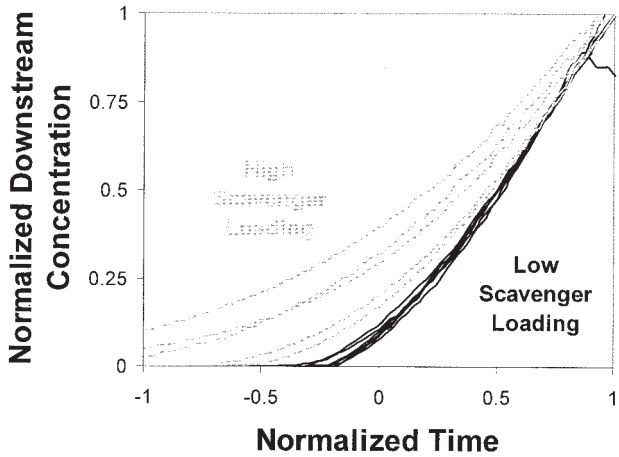

Figure 5. Normalized breakthrough curves for membranes with similarly large ZnO particles, slurried for 30 min before preparation.

The membranes contain different volume percentages (2.8%, gray lines; 1.2%, black lines) of ZnO.

Note that for the zinc oxide system, (kC_Y) equals $\{3\phi D/R^2\}$, as given in Eq. 4. These mass balances are subject to the constraints

$$C_X(z=0,\,t) = HC_{X0} \tag{9}$$

$$C_X(z,\,t=0) = 0 \tag{10}$$

$$C_X(z=\ell,\,t) = 0 \tag{11}$$

$$C_Y(z,\,t=0) = C_{Y0} \tag{12}$$

By nondimensionalizing our variables by

$$\tilde{C}_X = \frac{C_X}{HC_{X0}} \tag{13}$$

$$\tilde{C}_Y = \frac{C_Y}{C_{Y0}} \tag{14}$$

$$\tau = \frac{Dt}{\ell^2} \tag{15}$$

$$h = \frac{z}{\ell} \tag{16}$$

we find that the resulting system depends on only two parameters: a Damkohler number Φ

$$\Phi = \frac{kC_{Y0}\ell^2}{D} \tag{17}$$

and the scavenger loading γ,

$$\gamma = \frac{C_{Y0}}{\nu HC_{X0}} \tag{18}$$

The former is the ratio of the reaction rate to the diffusion rate; and the latter is the ratio of the initial scavenger concentration in the membrane to the solute concentration at the membrane's upstream interface.

These equations were solved numerically using standard centered finite-difference approximations and Euler method integration. The breakthrough curves, leakages, and kill times that are found are best expressed in dimensionless terms

$$\Lambda = \frac{L}{HC_{X0}A\ell}\left(\frac{D}{\ell^2}\right) \tag{19}$$

$$\tau_K = t_K\left(\frac{D}{\ell^2}\right) \tag{20}$$

$$\Theta_{\text{Max}} = \frac{Q_{\text{Max}}}{HC_{X0}A\ell} \tag{21}$$

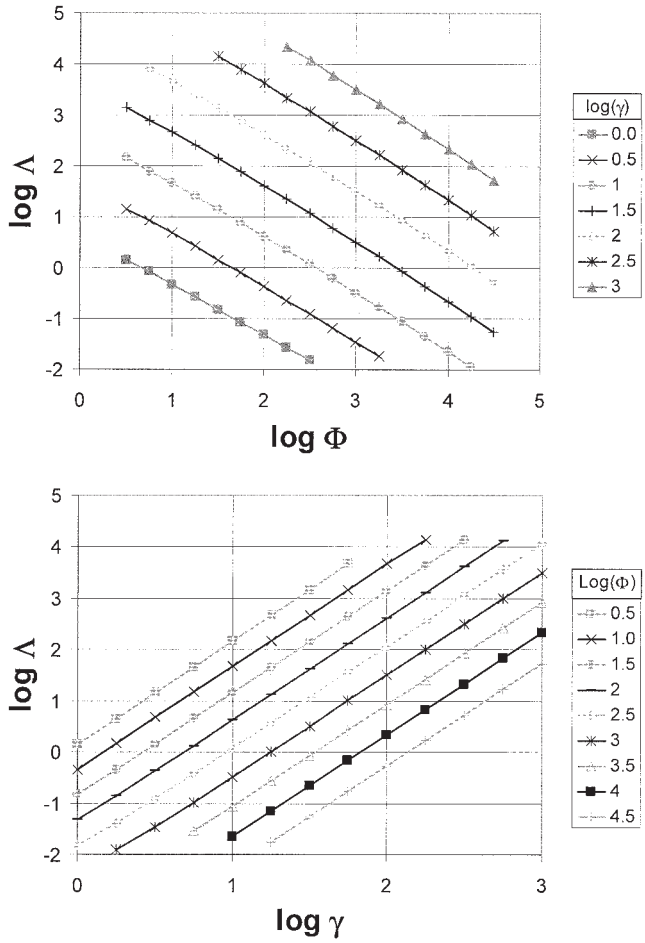

Figure 6. Dimensionless leakage Λ plotted against (a) reaction rate parameter Φ and (b) scavenger loading parameter γ.

The lines give clean linear regressions ($R^2 > 0.999$) with slopes of (a) -1.1 (RSD 4.8%) and (b) 2.0 (RSD 0.5%).

Figure 6 shows a clear logarithmic dependency of Λ on Φ and γ. This relationship can be accurately expressed by the following correlation

$$\Lambda = \alpha\gamma^2\Phi^{-1.1} \tag{22}$$

where α is a constant that, for these data, is approximately 5.

The correlation of the kill time is more complex because it depends on three parameters, Φ, γ, and Θ_{Max}. It does not have a simple linear dependency on these parameters, as we see plotting τ_K vs. log(Φ) at various values of γ in Figure 7. Instead, we see S-shaped curves, with plateaus at both high and low scavenger loadings. As the reaction rate approaches zero, the breakthrough curve behaves like that of a nonreactive membrane, approaching the reactive-membrane asymptote only after an infinitely long time. As the reaction rate approaches infinity, the breakthrough curve shifts almost instantly from $\Theta = 0$ to the steady-state asymptote. These limits of τ_K at large and small Φ can be expressed analytically as

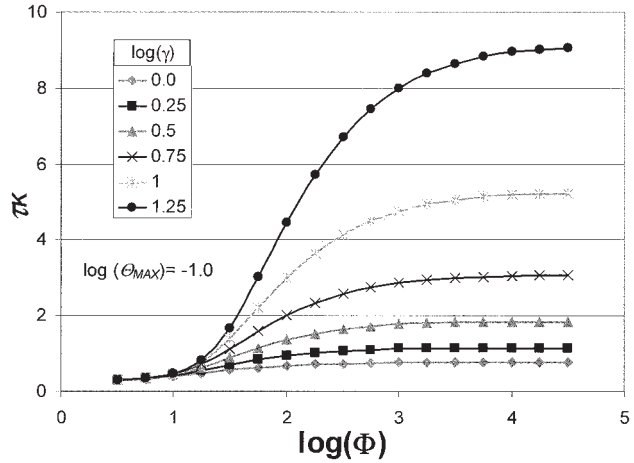

Figure 7. Dimensionless kill time τ_K transitions from a nonreactive value to an instantaneous reaction value as the reaction rate parameter Φ increases.

These values are described in Eqs. 23 and 24, with the latter limit dependent on scavenger loading γ.

$$\lim_{\Phi\to 0}\tau_K = \Theta_{\mathrm{Max}} + \frac{1}{6} + \frac{2}{\pi^2}\sum_{n=1}^{\infty}\frac{(-1)^n}{n^2}\exp\left(n^2\pi^2\lim_{\Phi\to 0}\tau_K\right) \qquad \text{(small } \Phi\text{)} \quad (23)$$

$$\lim_{\Phi\to\infty}\tau_K = \Theta_{\mathrm{Max}} + \frac{1}{6} + \frac{\gamma}{2} \qquad \text{(large } \Phi\text{)} \quad (24)$$

Our interest lies in the region of intermediate Φ values. Here, a small change in Φ can result in a large change in τ_K. Knowing the location of this "window of opportunity" will allow more intelligent design of reactive barrier membranes.

We can use our calculations to develop an analytic expression that predicts this window. One such expression, whose development is described elsewhere,[11] is plotted in Figure 8 against numeric data. We see that we can accurately predict the window over many orders of magnitude in Θ_{Max} and Φ (as well as γ) using the expression

$$\tau_K = \lim_{\Phi\to 0}\tau_K + \left(\lim_{\Phi\to\infty}\tau_K - \lim_{\Phi\to 0}\tau_K\right)\mathrm{erfo}\left\{3.75\left[\log\left(\frac{\gamma}{\Theta_{\mathrm{Max}}}\right) - 1.5\right]\Phi^{-1/2}\right\} \quad (25)$$

Note that if $\log(\gamma/\Theta_{Max})$ is less than 1.5, Eq. 25 cannot be evaluated. The fit deteriorates at small γ and large Θ_{Max}, a region of little practical interest. To obtain a useful estimate, $\log(\gamma/\Theta_{Max})$ should be at least 3.

Discussion

Our experiments showed that the leakage depends not only on the reaction rate (that is, on Φ) but also on the scavenger loading (that is, on γ). This unanticipated result, shown experimentally in Figure 5, is also indicated by our calculations, which show a greater dependency of leakage Λ on γ than on Φ. To examine this in more detail, we rewrite Eq. 22 for the dimensional L rather than Λ, approximating the (-1.1) exponent as (-1)

$$L = \left(\frac{A\ell}{\nu}\right)\alpha\,\frac{\gamma}{k} \quad (26)$$

The leakage L depends linearly on the scavenger loading and is inversely proportional to the reaction rate constant k. The γ dependency can be explained by the fact that the lag time increases linearly with the scavenger loading, so as γ increases, the time for solute to leak through also increases. In effect, increasing γ by a factor of 10 simply increases our timescale by a factor of 10, so we should expect a tenfold increase in the leakage, regardless of the reaction rate. Dividing L by γ, we have a breakthrough curve parameter that reflects only the reaction rate constant.

The lines in Figure 7 suggest an analytic pathway exists to our leakage expression, but our correlation for τ_K is not so precise. Nonetheless, it provides an accurate estimation of the "window of opportunity" over a large range of conditions without any additional fit parameters.

Perhaps the most remarkable attribute of the leakage and kill time correlations is their robustness. Returning to the ZnO system with which we experimented, we note that as the particles react, they shrink and their surface area per mass changes. To describe this system using Eqs. 7 and 8, we must allow our rate constant k, and thus our Damkohler number Φ, to change with time. However, because we have postulated that the reaction rate varies with ZnO surface area rather than with ZnO concentration, we can use the ZnO

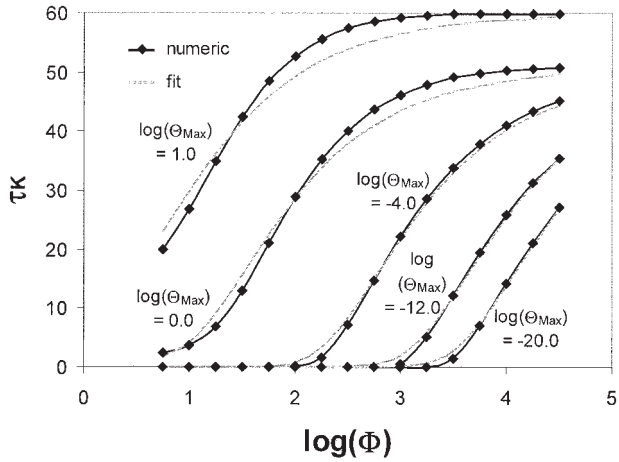

Figure 8. Transition of τ_K occurs at different Φ values as the kill concentration Θ_{Max} changes, with $\log(\gamma) = 2.0$.

Equation 25 (dashed) closely mimics numeric data (solid) over several orders of magnitude.

particle radius R rather than the ZnO concentration C_Y to write our reaction term, as demonstrated in Eq. 4. This leads to a significantly different kinetic model, as described in the Appendix. Performing similar calculations, however, we obtain almost identical correlations for the leakage and kill time.[11] The only differences are a factor of 3 decrease in α and an increase in the "3.75" of Eq. 26 by a factor of $(3)^{0.5}$. Both changes are consistent with an effective decrease in Φ by a factor of 3 because of the "3" prefactor in Eq. A1. As with Siegel's derivation for the steady-state asymptote, the nature of the kinetic expression appears to be irrelevant so long as the stoichiometry is defined.

Conclusions

The lag time of a barrier membrane can be dramatically increased by the addition of sacrificial scavengers. However, the lag time does not completely reflect transient solute transport, which may compromise the barrier's purpose. In addition to the permeability and the lag time, a third parameter is needed to quantify this transient solute transport. We have observed experimentally that this third parameter depends both on the reaction rate and on the amount of scavenger in the membrane, and we have constructed computer models that refine this relationship. We propose two candidates for this third parameter, the leakage Λ and the kill time τ_K, and have correlated them to known physical terms values. These correlations correspond well with our experiments, and so provide a stronger basis for rationally improving packaging.

Acknowledgments

E.E.N. is grateful for a National Science Foundation Graduate Research Fellowship. The research was chiefly supported by the Air Force Office of Scientific Research (Grant F4960-01-1-0333) and by the U.S. Department of Energy (Grant DE-FG07-02ER63509). Other support came from the Petroleum Research Fund (Grant 39083-AC9) and from the National Science Foundation (Grant CTS 0322882).

Notation

A = membrane area
C = species concentration
$\tilde{C}$ = dimensionless species concentration
D = diffusion coefficient
h = dimensionless membrane coordinate, $h = z/\ell$
H = partition coefficient
k = reaction rate constant
ℓ = membrane thickness
L = leakage
MW = molecular weight
Q = total amount of solute which has entered package
R = scavenger particle radius
$\tilde{R}$ = dimensionless scavenger particle radius
t = time
X = solute name
Y = scavenger name
z = membrane coordinate

Greek letters

α = constant
ϕ = scavenger volume fraction
Φ = Damkohler number
γ = dimensionless scavenger loading, $\gamma = C_Y/C_{Y0}$
Λ = dimensionless leakage, $\Lambda = L(D/HC_{X0}A\ell^3)$
ν = stoichiometric coefficient
Θ = dimensionless total amount of solute which has entered package, $\Theta = Q/HC_{X0}A\ell$
ρ = density
τ = dimensionless time

Subscripts

K = refers to kill time
L = refers to lag time
Max = refers to parameter value at kill time
0 = refers to initial value
X = refers to solute X
Y = refers to scavenger Y

Literature Cited

1. Crank J. *The Mathematics of Diffusion.* Oxford, UK: Clarendon Press; 1975.
2. Daynes HA. The process of diffusion through a rubber membrane. *Proceedings of the Royal Society of London Series A—Mathematical and Physical Sciences.* 1920;A97:286-307.
3. Siegel RA, Cussler EL. Reactive barrier membranes: Some theoretical observations regarding the time lag and breakthrough curves. *Journal of Membrane Science*. 2004;229:33-41.
4. Finger KF, Lemberger AP, Higuchi T, Busse LW, Wurster DE. Investigation and development of protective ointments IV. *Journal of the American Pharmaceutical Association*. 1960;49:569-573.
5. Higuchi WI, Higuchi T. Theoretical analysis of diffusional movement through heterogeneous barriers. *Journal of the American Pharmaceutical Association*. 1960;49:598-606.
6. Higuchi T. Rate of release of medicaments from ointment bases containing drugs in suspension. *Journal of Pharmaceutical Sciences*. 1961;50:874-875.
7. Paul DR. Effect of immobilizing adsorption on diffusion time lag. *Journal of Polymer Science Part A2: Polymer Physics*. 1961;7:1811-1818.
8. Paul DR, Kemp DR. The diffusion time lag in polymer membranes containing adsorptive fillers. *Journal of Polymer Science Polymer Symposia*. 1973;41:79-93.
9. Paul DR, Koros WJ. Effect of partially immobilizing sorption on permeability and the diffusion time lag. *Journal of Polymer Science Polymer Physics Education*. 1976;14:675-685.
10. Yang C, Nuxoll EE, Cussler EL. Reactive barrier films. *AIChE Journal*. 2001;47:295-302.
11. Nuxoll EE. *Transient Transport in Reactive Barrier Membranes.* PhD Thesis. Minneapolis, MN: University of Minnesota; 2003.
12. Cussler EL. *Diffusion and Mass Transport in Fluid Systems*. 2nd ed. New York, NY: Cambridge Univ. Press; 1997.
13. Libby B, Smyrl WH, Cussler EL. Polymer–zeolite composite membranes for direct methanol fuel cells. *AIChE Journal.* 2003;49:991-1001.

Appendix

Using the rate expression for a reactive particle given in Eq. 4, we can rewrite Eqs. 7 and 8 in terms of C_X and R, replacing scavenger concentration C_Y with particle radius R as our second dependent variable. If we assume that $R \ll \ell$ and $\phi \ll 1$, then

$$\frac{\partial C_X}{\partial t} = D\,\frac{\partial^2 C_X}{\partial z^2} - \frac{3D\phi}{R_0^2}\left(\frac{R}{R_0}\right)C_X \tag{A1}$$

$$\frac{\partial R}{\partial t} = -\frac{\nu D M W_Y C_X}{\rho_Y R} \tag{A2}$$

Note that the time derivative of R varies inversely with R; that is, the smaller a particle becomes, the faster it shrinks. This

system, although using a substantially different kinetic expression, is still dependent on two parameters

$$\Phi = \frac{\phi \ell^2}{R_0^2} \tag{A3}$$

$$\gamma = \frac{\phi \rho_Y}{\nu M W_Y H C_{X0}} = \frac{C_{Y0}}{\nu H C_{X0}} \tag{A4}$$

The membrane loading γ is the same as before. Our Damkohler number, although still a ratio of the effective reaction rate to the diffusion rate, no longer contains a rate constant, either k or D. Because our effective reaction rate is actually a second diffusion rate, according to Eq. 6, the ratio of rates is simply a ratio of the length scales of our diffusion processes.

Manuscript received Oct. 7, 2003, and revision received May 28, 2004.